energies

MDPI

Article

Reconfigurable Intelligent Surface-Assisted Secure Communication in Cognitive Radio Systems

Xinshui Wang [1,*], Xu Wang [1], Jimin Ge [1], Zhibin Liu [1], Yuefeng Ma [1] and Xingwang Li [2]

[1] School of Computer Science, Qufu Normal University, Rizhao 276826, China
[2] School of Physics and Electronic Information Engineering, Henan Polytechnic University, Jiaozuo 454099, China
* Correspondence: wxinshui@126.com

Abstract: A reconfigurable intelligent reflective surface (RIS)-assisted cognitive radio (CR) multiple-input multiple-output (MIMO) secure communication system is considered. In the presence of an eavesdropper, a primary base station (PBS) and a cognitive base station (CBS) equipped with multiple antennas communicate to a primary user (PU) and a secondary user (SU), respectively. In order to maximize the achievable secrecy rate of the system, the secrecy rate maximization problem is first transformed into a secure energy efficiency (SEE) problem using an objective function. Then, the security energy efficiency of the system is maximized by jointly optimizing the transmit beam formation of the base station and the reflected beam formation of the smart reflecting surface under the conditions that the total transmitted power constraint and the interference power constraint are satisfied. To address the difficulty in solving the resulting optimization problem, we apply an algorithm based on alternating optimization and semidefinite relaxation, as well as Dinklbach's algorithm, to solve the problem. Simulation results show that this method can significantly improve the safety energy efficiency of the system.

Keywords: intelligent reflective surfaces; physical layer security; cognitive radio

Citation: Wang, X.; Wang, X.; Ge, J.; Liu, Z.; Ma, Y.; Li, X. Reconfigurable Intelligent Surface-Assisted Secure Communication in Cognitive Radio Systems. *Energies* **2024**, *17*, 515. https://doi.org/10.3390/en17020515

Academic Editor: Daniele D. Giusto

Received: 7 November 2023
Revised: 14 January 2024
Accepted: 17 January 2024
Published: 20 January 2024

1. Introduction

In the era of rapid development, the proliferation of emerging applications has resulted in a substantial upsurge in the demand for network communication traffic. While 5G communication systems exhibit noteworthy advancements over their predecessors [1], forthcoming wireless communications necessitate even higher throughput, enhanced security, reduced latency, lower energy consumption, extensive connectivity, network densification, and improved Quality of Service (QoS) [2]. Additionally, the exponential growth of numerous emerging mobile application models and the surge in network traffic will engender an immense and escalating need for the radio spectrum. To effectively cope with the burgeoning mobile data traffic in future wireless network communications, it is imperative to address the scarcity of spectrum resources [3].

Cognitive Radio Network (CRN) is widely acknowledged as a promising solution to enhance the efficient utilization of spectrum resources. CRN utilizes dynamic spectrum access and reconfiguration, enabling it to comprehend its surroundings and adapt its operating parameters according to the changes in the radio frequency (RF) environment. This breakthrough innovation in radio technology, Cognitive Radio (CR), paves the way for significant improvements in the utilization of congested radio spectra [4].

In CRN systems, CR serves as an effective technique to enhance Spectrum Efficiency (SE), and its users are classified into PU and SU. A PU is a licensed user who possesses higher priority in accessing the spectrum. On the other hand, an SU is typically an unlicensed user who can share the spectrum of the PU while ensuring that no harmful interference is caused to the PU [5]. For secondary users, the primary concern is to share

the spectrum of the PU while minimizing interference and maintaining QoS for themselves, thereby maximizing spectrum efficiency.

While CRNs offer significant improvements in the spectral efficiency of wireless networks, they also face challenges related to optimizing performance for both PUs and SUs, as well as ensuring robust security [6]. Practical applications of CRNs encounter persistent obstacles concerning network energy consumption and hardware costs. Additionally, like traditional wireless networks, CRNs are susceptible to security issues. As previously mentioned, the ability of the physical layer in CRNs to sense and comprehend the surrounding RF environment becomes a vulnerability that adversaries can exploit for malicious activities.

The dynamic and open nature of the physical layer in CRNs renders cognitive communications highly vulnerable to various internal and external malicious activities. In recent years, numerous research efforts have focused on developing secure transmission techniques at the physical layer specifically tailored for CRNs. These techniques include Artificial Noise (AN)-assisted beamforming, Cooperative Jamming (CJ), and Cooperative Relaying schemes [7]. However, these approaches primarily concentrate on signal processing at the receiver and transmitter to adapt to changes in the wireless environment. They are unable to completely mitigate the negative effects caused by the uncontrollable electromagnetic wave propagation environment. Moreover, the deployment of a large number of relays in a secure wireless system inevitably leads to excessive costs. Additionally, collaborative interference and artificial noise introduce additional power consumption. Considering the limitations of these existing approaches, there is an urgent need for a new wireless security paradigm that is both cost-effective and energy-efficient.

In recent years, the emergence of Intelligent Reflecting Surface (RIS) technology, made possible by advancements in technology and metamaterials, has provided new opportunities. RIS is a planar array comprising numerous reconfigurable passive elements, each capable of independently modulating the incident signal to induce a specific phase shift. This collective manipulation of the reflected signal's propagation characteristics enables RIS to significantly enhance the spectral efficiency and security of wireless networks at a low cost [8]. RIS technology offers a high level of flexibility for resource allocation and CRN systems. Moreover, researchers have started exploring the application of RIS to enhance the physical layer security of wireless communications. By adjusting the phase shift of the reflected signals, RIS can reshape the wireless propagation environment. This adjustment increases the data rate for legitimate receivers while decreasing the data rate for potential eavesdroppers, thereby reducing information leakage and enhancing overall system security [9]. Consequently, the integration of RIS into CRN systems holds promise as a solution to address the challenges faced by CRNs, improving spectral efficiency and energy efficiency, and facilitating green and secure communications.

1.1. Related Work

Reference [10] focused on a MISO CR system and demonstrates the benefits of beamforming in increasing the secrecy rate. Reference [11] considered a MIMO CR network and introduced a robust secure beamforming design to obtain the maximum achievable secrecy rate for the worst-case SU. Furthermore, several scholars have utilized various auxiliary techniques, such as the introduction of AN, relaying, and Collaborative Jamming to enhance the secure transmission performance of CR communication systems. In reference [12], AN was introduced to enhance secure communication in fast-fading environments for SUs. Reference [13] explored secure transmission in CR networks using relay-assisted orthogonal frequency division multiple access, considering latent eavesdroppers. Additionally, reference [14] investigated bidirectional relaying in CR communication systems, showing significant improvements in secrecy and rate for SUs. Moreover, reference [15] proposed a wireless energy-harvesting Collaborative Jammer-assisted transmission scheme to enhance CR system security. However, these studies have two main drawbacks. Firstly, deploying relays or auxiliary devices for secure output incurs high hardware costs and additional energy consumption. Secondly, ensuring satisfactory confidentiality perfor-

mance in harsh wireless transmission environments remains challenging, even with AN or jamming signals.

The above energy consumption problems can be addressed well by introducing an RIS in CR networks. Due to full-duplex transmission and low power consumption, RIS has received a great deal of attention from both academia and industry as a promising technology that can significantly improve energy efficiency in 6G communications. It is a new cost-effective and energy-efficient technology that can shape the radio propagation environment and is well-suited to improve the energy efficiency of CR systems. In reference [16], RIS was proposed as a means to enhance the data transfer rate of SUs in MIMO CR systems. Reference [17] investigated RIS-assisted MISO CR systems to maximize the transmission rate of SUs. However, security considerations were not addressed. Subsequent studies focused on the security aspect. In reference [18], the authors examined the security performance of RIS-assisted underlay-mode CR systems, enhancing the secrecy rate of SUs. In reference [19], the problem of improving SUs' secrecy in the presence of multiple eavesdroppers was investigated. The extension to the MIMO model was explored in reference [20] to maximize SUs' secrecy rate with RIS. However, the trade-off between secrecy rate and energy consumption was considered in reference [21], aiming to maximize the Secrecy Energy Efficiency (SEE) of SUs by utilizing RIS.

1.2. Contributions

However, the aforementioned studies primarily focused on the secrecy rate and energy consumption of SU, neglecting the security and energy consumption aspects of the entire CR system in the presence of PU. Therefore, building upon the existing research, we propose a novel communication scenario to address the secure communication problem in the downlink and introduce the concept of an RIS to enhance the secure communication performance of the entire CR system. The main contributions of our work are as follows:

- In a novel CR downlink communication scenario, a PBS communicates with a PU, while a CBS communicates with a SU. The entire CR system is subject to eavesdropping by an external entity;
- We balance the secrecy rate and energy consumption by formulating a secure energy efficiency objective function, transforming the maximization of secrecy rate into a secure energy efficiency problem;
- To efficiently solve the non-convex objective function in the subproblem, we employ an SCA-like (Sequential Convex Approximation-like) lemma. This approach helps overcome the nonconvexity and enables effective optimization of the objective function;
- We propose an efficient algorithm based on alternating optimization, semidefinite relaxation, and Dinklbach's method to solve the resulting optimization problem. Our method effectively improves the safety energy efficiency of the overall CR system, as demonstrated by simulation results.

2. System Model and Problem

2.1. System Model

As shown in Figure 1, an RIS-assisted CR MIMO communication system model is considered. The PBS with M_p antenna and the CBS with M_c antenna communicate with the PU and the SU, each with a single antenna, respectively. Also, the user PU and SU are subject to interference. In the depicted scenario, the eavesdropper (Eve) is equipped with a single antenna, while the RIS comprises N passive reflective elements. During the transmission of confidential messages by the PBS and CBS, the PU receives both useful signals from PBS and RIS, as well as interfering signals from CBS and their reflections by RIS. The SU experiences a similar situation. Eve attempts to eavesdrop on all users. It is assumed that all channels within the system undergo quasi-static flat fading. The channel matrices from PBS to RIS, from PBS to PU, from PBS to SU, from PBS to Eve, and from RIS to Eve and RIS to PU are denoted by $\mathbf{G}_{\mathrm{p}} \in \mathbb{C}^{M_p \times N}$, $\mathbf{h}_{\mathrm{pp}} \in \mathbb{C}^{M_p \times 1}$, $\mathbf{h}_{\mathrm{ps}} \in \mathbb{C}^{M_p \times 1}$, $\mathbf{h}_{\mathrm{pe}} \in \mathbb{C}^{M_p \times 1}$, and $\mathbf{h}_{\mathrm{re}} \in \mathbb{C}^{N \times 1}$, respectively. The channel matrices from CBS to RIS, from CBS to SU, from

CBS to PU, from CBS to Eve, and from RIS to SU are denoted by $\mathbf{G}_{\mathrm{c}} \in \mathbb{C}^{M_c \times N}$, $\mathbf{h}_{\mathrm{cp}} \in \mathbb{C}^{M_c \times 1}$, $\mathbf{h}_{\mathrm{cs}} \in \mathbb{C}^{M_c \times 1}$, and $\mathbf{h}_{\mathrm{ce}} \in \mathbb{C}^{M_c \times 1}$, respectively.

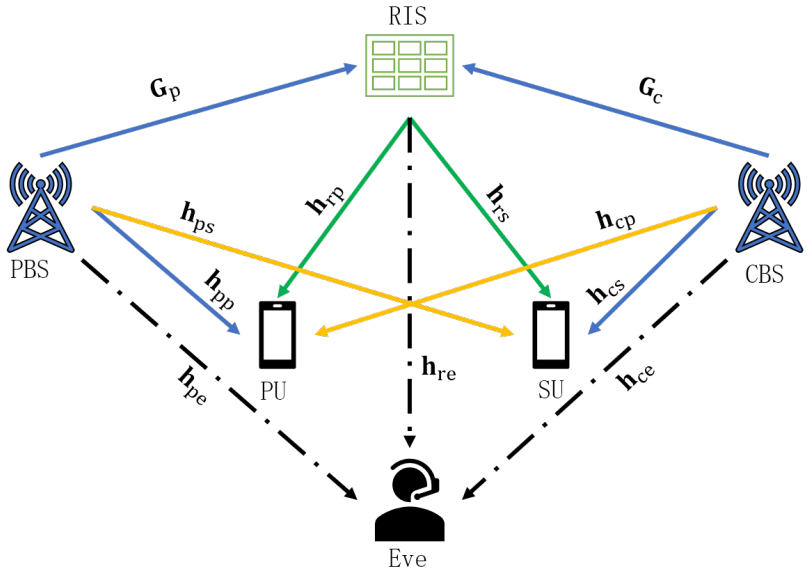

Figure 1. RIS-assisted Cognitive Radio Network.

We assume that all channels experience quasi-static flat fading and that the channel state information (CSI) is completely known for all channels. Using the received signals of PU and SU, Eve can be expressed as

$$y_p = \left(\mathbf{h}_{\mathrm{pp}}^H + \mathbf{h}_{\mathrm{rp}}^H \mathbf{\Phi} \mathbf{G}_{\mathrm{p}}\right) \mathbf{f}_{\mathrm{p}} x_{\mathrm{p}} + \left(\mathbf{h}_{\mathrm{cp}}^H + \mathbf{h}_{\mathrm{rp}}^H \mathbf{\Phi} \mathbf{G}_{\mathrm{c}}\right) \mathbf{f}_{\mathrm{c}} x_{\mathrm{c}} + n_{\mathrm{e}} \tag{1}$$

$$y_s = \left(\mathbf{h}_{\mathrm{cs}}^H + \mathbf{h}_{\mathrm{rs}}^H \mathbf{\Phi} \mathbf{G}_{\mathrm{c}}\right) \mathbf{f}_{\mathrm{c}} x_{\mathrm{c}} + \left(\mathbf{h}_{\mathrm{ps}}^H + \mathbf{h}_{\mathrm{rs}}^H \mathbf{\Phi} \mathbf{G}_{\mathrm{p}}\right) \mathbf{f}_{\mathrm{p}} x_{\mathrm{p}} + n_{\mathrm{s}} \tag{2}$$

$$y_e = \left(\mathbf{h}_{\mathrm{pe}}^H + \mathbf{h}_{\mathrm{re}}^H \mathbf{\Phi} \mathbf{G}_{\mathrm{p}}\right) \mathbf{f}_{\mathrm{p}} x_{\mathrm{p}} + \left(\mathbf{h}_{\mathrm{ce}}^H + \mathbf{h}_{\mathrm{re}}^H \mathbf{\Phi} \mathbf{G}_{\mathrm{c}}\right) \mathbf{f}_{\mathrm{c}} x_{\mathrm{c}} + n_{\mathrm{e}} \tag{3}$$

where the superscript H denotes the conjugate transpose operation. The phase shift matrix of RIS is denoted by $\mathbf{\Phi} = \mathrm{diag}\left(e^{j\theta_1}, \ldots, e^{j\theta_n}\right)$, $\theta_n \in [0, 2\pi]$. Let $q_n = e^{j\theta_n}$, in order to maximize the reflected power gain; then, q_n should satisfy

$$|q_n| = 1, \quad \forall \mathrm{n} \tag{4}$$

$\mathbf{f}_{\mathrm{p}}$ and $\mathbf{f}_{\mathrm{c}}$ are the transmit beamforming vectors of the PBS and CBS of the base station satisfying $\left\|\mathbf{f}_{\mathrm{p}}\right\|^2 \leq P_p^{\max}$ and $\left\|\mathbf{f}_{\mathrm{c}}\right\|^2 \leq P_c^{\max}$, respectively, where $\|\cdot\|$ denotes the Euclidean parametrization and $P^{\max}$ denotes the maximum transmission power of the base station. x_p and x_c are complex Gaussian random variables with mean 0. $\mathbb{E}\{|x|^2\} = 1$, n_p, n_s and n_e denote the additive Gaussian white noise at PU, SU, and Eve, respectively, with zero mean and variance σ_p^2, σ_s^2, and σ_e^2, respectively. Thus, the achievable rates of PU and SU can be specified as

$$R_p = \log_2\left(1 + \frac{\left|\left(\mathbf{h}_{\mathrm{pp}}^H + \mathbf{h}_{rp}^H \mathbf{\Phi} \mathbf{G}_{\mathrm{p}}\right) \mathbf{f}_{\mathrm{p}}\right|^2}{\left|\left(\mathbf{h}_{\mathrm{cp}}^H + \mathbf{h}_{\mathrm{rp}}^H \mathbf{\Phi} \mathbf{G}_{\mathrm{c}}\right) \mathbf{f}_{\mathrm{c}}\right|^2 + \sigma_p^2}\right) \tag{5}$$

$$R_s = \log_2\left(1 + \frac{\left|\left(\mathbf{h}_{\mathrm{cs}}^H + \mathbf{h}_{rs}^H \mathbf{\Phi} \mathbf{G}_{\mathrm{c}}\right) \mathbf{f}_{\mathrm{c}}\right|^2}{\left|\left(\mathbf{h}_{\mathrm{ps}}^H + \mathbf{h}_{\mathrm{rs}}^H \mathbf{\Phi} \mathbf{G}_{\mathrm{p}}\right) \mathbf{f}_{\mathrm{p}}\right|^2 + \sigma_s^2}\right) \tag{6}$$

The achievable rates of the eavesdropping links from Eve to PU and SU, respectively, are

$$R_{e,p} = \log_2\left(1 + \frac{\left|\left(\mathbf{h}_{\mathrm{pe}}^H + \mathbf{h}_{\mathrm{re}}^H \mathbf{\Phi} \mathbf{G}_{\mathrm{p}}\right)\mathbf{f}_{\mathrm{p}}\right|^2}{\left|(\mathbf{h}_{\mathrm{ce}}^H + \mathbf{h}_{\mathrm{re}}^H \mathbf{\Phi} \mathbf{G}_{\mathrm{c}})\mathbf{f}_{\mathrm{c}}\right|^2 + \sigma_e^2}\right) \tag{7}$$

$$R_{e,s} = \log_2\left(1 + \frac{\left|\left(\mathbf{h}_{\mathrm{ce}}^H + \mathbf{h}_{\mathrm{re}}^H \mathbf{\Phi} \mathbf{G}_{\mathrm{c}}\right)\mathbf{f}_{\mathrm{c}}\right|^2}{\left|\left(\mathbf{h}_{\mathrm{pe}}^H + \mathbf{h}_{\mathrm{re}}^H \mathbf{\Phi} \mathbf{G}_{\mathrm{p}}\right)\mathbf{f}_{\mathrm{p}}\right|^2 + \sigma_e^2}\right) \tag{8}$$

The secrecy rate (SR) from PBS to PU is

$$R_{sec,p} = \left[R_p - R_{e,p}\right]^+ \tag{9}$$

The secrecy rate from CBS to SU is

$$R_{sec,s} = \left[R_s - R_{e,s}\right]^+ \tag{10}$$

where $[\mathrm{z}]^+ = \max(0, x)$. Since the maximum SR must be non-negative, the $[\cdot]^+$ operation can be omitted without loss of optimality. The total power consumption of the system, P_{total} , consists of both the transmitted power and the dissipation of the hardware components:

$$P_{\mathrm{total}} = \left\|\mathbf{f}_{\mathrm{p}}\right\|^2 + \left\|\mathbf{f}_{\mathrm{c}}\right\|^2 + NP_{\mathrm{dyn}} + P_{sta} + P_{su}^{cir} + P_{pu}^{cir} + P_{BS}^{cir} \tag{11}$$

where $\left\|\mathbf{f}_{\mathrm{p}}\right\|^2$ and $\left\|\mathbf{f}_{\mathrm{c}}\right\|^2$ denote the transmitted power consumption energy of the PBS and CBS of the base station, respectively. P_{dyn} denotes the dynamic power consumption of each reflective element of the RIS, N represents the number of RIS reflection elements, P_{sta} denotes the static power required to maintain the basic circuit operation of the RIS, and $P_{\mathrm{su}}^{\mathrm{cir}}$, $P_{\mathrm{pu}}^{\mathrm{cir}}$, and $P_{\mathrm{BS}}^{\mathrm{cir}}$ denote the user SU and PU and the hardware power consumed by the base station, respectively. In summary, we define the safe energy efficiency of the system as

$$\eta = \left(R_{\mathrm{sec},p} + R_{\mathrm{sec,s}}\right)/P_{\mathrm{total}} \tag{12}$$

At the same time, during the cognitive transmission, the interference temperature to PU must be lower than a predefined threshold I_{th} to ensure the QoS of PU, i.e.,

$$\left|\left(\mathbf{h}_{\mathrm{cp}}^H + \mathbf{h}_{\mathrm{rp}}^H \mathbf{\Phi} \mathbf{G}_{\mathrm{c}}\right)\mathbf{f}_{\mathrm{c}}\right|^2 \leq I_{th} \tag{13}$$

2.2. Problem Formulation

Under this condition, the objective of this paper is to maximize η by jointly optimizing the reflection phase shift matrix $\mathbf{\Phi}$ and the transmitted beamforming vectors $\mathbf{f}_{\mathrm{p}}$ and $\mathbf{f}_{\mathrm{c}}$, using the equation. We obtain the following equivalent formulation of Problem (1):

$$\max_{\mathbf{f}_{\mathrm{p}}, \mathbf{f}_{\mathrm{c}}, \mathbf{\Phi}} \quad \eta \tag{14}$$

$$s.t. \quad \left\|\mathbf{f}_{\mathrm{p}}\right\|^2 \leq P_{\mathrm{p}}^{\max} \tag{14a}$$

$$\left\|\mathbf{f}_{\mathrm{c}}\right\|^2 \leq P_{\mathrm{c}}^{\max} \tag{14b}$$

$$|\mathrm{q}_n| = 1, \quad \forall \mathrm{n} \tag{14c}$$

$$\left|\left(\mathbf{h}_{\mathrm{cp}}^H + \mathbf{h}_{\mathrm{rp}}^H \mathbf{\Phi} \mathbf{G}_{\mathrm{c}}\right)\mathbf{f}_{\mathrm{c}}\right|^2 \leq I_{th} \tag{14d}$$

$P_{\mathrm{p}}^{\max}$ and $P_{\mathrm{c}}^{\max}$ denote the maximum transmitted power of the base station CBS and PBS, respectively. Obviously, (P1) is difficult to solve due to the nonconvex objective function as well as the coupled optimization variables. Therefore, in this paper, we apply an AO-based algorithm to solve (P1). By iteratively optimizing one of $\left(\mathbf{f}_{\mathrm{c}}, \mathbf{f}_{\mathrm{p}}\right)$, and $\mathbf{\Phi}$, the other is fixed in each iteration until convergence is reached, as detailed below.

3. Alternating Optimization-Based Algorithm

3.1. Given $\mathbf{\Phi}$*, Optimize* $\left(\mathbf{f}_{\mathrm{c}}, \mathbf{f}_{\mathrm{p}}\right)$

First, we define the following symbols below:

$\mathbf{h}_{\mathrm{p1}} = \mathbf{h}_{\mathrm{pp}}^H + \mathbf{h}_{\mathrm{rp}}^H \boldsymbol{\Phi} \mathbf{G}_{\mathrm{p}}$, $\mathbf{H}_{\mathrm{p1}} = \mathbf{h}_{\mathrm{p1}}^H \mathbf{h}_{\mathrm{p1}}$.
$\mathbf{h}_{\mathrm{p2}} = \mathbf{h}_{\mathrm{cp}}^H + \mathbf{h}_{\mathrm{rp}}^H \boldsymbol{\Phi} \mathbf{G}_{\mathrm{c}}$, $\mathbf{H}_{\mathrm{p2}} = \mathbf{h}_{\mathrm{p2}}^H \mathbf{h}_{\mathrm{p2}}$.
$\mathbf{h}_{\mathrm{s1}} = \mathbf{h}_{\mathrm{cs}}^H + \mathbf{h}_{\mathrm{rs}}^H \boldsymbol{\Phi} \mathbf{G}_{\mathrm{c}}$, $\mathbf{H}_{\mathrm{s1}} = \mathbf{h}_{\mathrm{s1}}^H \mathbf{h}_{\mathrm{s1}}$.
$\mathbf{h}_{\mathrm{s2}} = \mathbf{h}_{\mathrm{ps}}^H + \mathbf{h}_{\mathrm{rs}}^H \boldsymbol{\Phi} \mathbf{G}_{\mathrm{p}}$, $\mathbf{H}_{\mathrm{s2}} = \mathbf{h}_{\mathrm{s2}}^H \mathbf{h}_{\mathrm{s2}}$.
$\mathbf{h}_{\mathrm{e1}} = \mathbf{h}_{\mathrm{pe}}^H + \mathbf{h}_{\mathrm{re}}^H \boldsymbol{\Phi} \mathbf{G}_{\mathrm{p}}$, $\mathbf{H}_{\mathrm{e1}} = \mathbf{h}_{\mathrm{e1}}^H \mathbf{h}_{\mathrm{e1}}$.
$\mathbf{h}_{\mathrm{e2}} = \mathbf{h}_{\mathrm{ce}}^H + \mathbf{h}_{\mathrm{re}}^H \boldsymbol{\Phi} \mathbf{G}_{\mathrm{c}}$, $\mathbf{H}_{\mathrm{e2}} = \mathbf{h}_{\mathrm{e2}}^H \mathbf{h}_{\mathrm{e2}}$.
$\mathbf{F}_{\mathrm{c}} = \mathbf{f}_{\mathrm{c}} \mathbf{f}_{\mathrm{c}}^H, \quad \mathbf{F}_{\mathrm{P}} = \mathbf{f}_{\mathrm{P}} \mathbf{f}_{\mathrm{P}}^H$

Then, Equation (5) can be simplified to

$$R_p = \log_2 \left(1 + \frac{\mathbf{h}_{\mathrm{p1}} \mathbf{F}_{\mathrm{p}} \mathbf{h}_{\mathrm{p1}}^H}{\mathbf{h}_{\mathrm{p2}} \mathbf{F}_{\mathrm{c}} \mathbf{h}_{\mathrm{p2}}^H + \sigma_p^2} \right) \tag{15}$$

Let tr(Z) and rank(Z) denote the trace and rank of the matrix Z, respectively, where the semidefinite relaxation (SDR) algorithm [22] is applied. Equation (15) can be written as

$$R_p = \log_2 \left(1 + \frac{\mathrm{tr}\left(\mathbf{H}_{\mathrm{p}_1} \mathbf{F}_{\mathrm{p}}\right)}{\mathrm{tr}\left(\mathbf{H}_{\mathrm{p}_2} \mathbf{F}_{\mathrm{C}}\right) + \sigma_p^2} \right) \tag{16}$$

Further,

$$R_p = \log_2 \left(\frac{\lambda_p \,\mathrm{tr}\left(\mathbf{H}_{\mathrm{p2}} \mathbf{F}_{\mathrm{c}}\right) + \lambda_p \,\mathrm{tr}\left(\mathbf{H}_{\mathrm{p1}} \mathbf{F}_{\mathrm{p}}\right) + 1}{\lambda_p \,\mathrm{tr}\left(\mathbf{H}_{\mathrm{p2}} \mathbf{F}_{\mathrm{c}}\right) + 1} \right), \lambda_p = 1/\sigma_p^2 \tag{17}$$

Similarly, we can obtain

$$R_S = \log_2 \left(\frac{\lambda_s \,\mathrm{tr}\left(\mathbf{H}_{\mathrm{s2}} \mathbf{F}_{\mathrm{p}}\right) + \lambda_s \,\mathrm{tr}(\mathbf{H}_{\mathrm{s1}} \mathbf{F}_{\mathrm{C}}) + 1}{\lambda_p \,\mathrm{tr}\left(\mathbf{H}_{\mathrm{s2}} \mathbf{F}_{\mathrm{p}}\right) + 1} \right), \lambda_s = 1/\sigma_S^2 \tag{18}$$

$$R_{e,p} = \log_2 \left(\frac{\lambda_e \,\mathrm{tr}(\mathbf{H}_{\mathrm{e2}} \mathbf{F}_{\mathrm{C}}) + \lambda_e \,\mathrm{tr}\left(\mathbf{H}_{\mathrm{e1}} \mathbf{F}_{\mathrm{p}}\right) + 1}{\lambda_e \,\mathrm{tr}(\mathbf{H}_{\mathrm{e2}} \mathbf{F}_{\mathrm{C}}) + 1} \right), \lambda_e = 1/\sigma_e^2 \tag{19}$$

$$R_{e,s} = \log_2 \left(\frac{\lambda_e \,\mathrm{tr}\left(\mathbf{H}_{\mathrm{e1}} \mathbf{F}_{\mathrm{p}}\right) + \lambda_e \,\mathrm{tr}(\mathbf{H}_{\mathrm{e2}} \mathbf{F}_{\mathrm{c}}) + 1}{\lambda_e \,\mathrm{tr}\left(\mathbf{H}_{\mathrm{e1}} \mathbf{F}_{\mathrm{p}}\right) + 1} \right), \lambda_e = 1/\sigma_e^2 \tag{20}$$

To further address the nonconvexity of the objective function, we quote the following lemma [23].

Lemma 1. *For any $x > 0$, consider the function $\varphi(t) = -tx + \ln t + 1$. Then, we have*

$$-\ln x = \max_{t>0} \varphi(t) \tag{21}$$

The optimal solution is $t = 1/x$. Lemma 1 provides an upper bound for $\varphi(t)$, which is tight when $t = 1/x$. For R_p, applying Lemma 1, let $x = \lambda_p \,\mathrm{tr}\left(\mathbf{H}_{\mathrm{p2}} \mathbf{F}_{\mathrm{c}}\right) + 1$ and $t = t_p$; then, R_p can be written as

$$\begin{aligned} R_p \ln 2 &= \ln\left(\lambda_p \,\mathrm{tr}\left(\mathbf{H}_{\mathrm{p2}} \mathbf{F}_{\mathrm{c}}\right) + \lambda_p \,\mathrm{tr}\left(\mathbf{H}_{\mathrm{p1}} \mathbf{F}_{\mathrm{p}}\right) + 1\right) - \ln\left(\lambda_p \,\mathrm{tr}\left(\mathbf{H}_{\mathrm{p2}} \mathbf{F}_{\mathrm{c}}\right) + 1\right) \\ &= \max_{t_p>0} \varphi_p\left(\mathbf{F}_{\mathrm{p}}, \mathbf{F}_{\mathrm{c}}, t_p\right) \end{aligned} \tag{22}$$

where

$$\begin{aligned} \varphi_p\left(\mathbf{F}_{\mathrm{p}}, \mathbf{F}_{\mathrm{c}}, t_p\right) = &\ln\left(\lambda_p \,\mathrm{tr}\left(\mathbf{H}_{\mathrm{p2}} \mathbf{F}_{\mathrm{c}}\right) + \lambda_p \,\mathrm{tr}\left(\mathbf{H}_{\mathrm{p1}} \mathbf{F}_{\mathrm{p}}\right) + 1\right) \\ &- t_p\left(\lambda_p \,\mathrm{tr}\left(\mathbf{H}_{\mathrm{p2}} \mathbf{F}_{\mathrm{c}}\right) + 1\right) + \ln t_p + 1 \end{aligned} \tag{23}$$

Similarly, we set $x = \lambda_s \,\mathrm{tr}\left(\mathbf{H}_{\mathrm{s2}} \mathbf{F}_{\mathrm{p}}\right) + 1$ and $t = t_s$, and R_s can then be written as

$$\begin{aligned} R_s \ln 2 &= \ln\left(\lambda_s \,\mathrm{tr}\left(\mathbf{H}_{\mathrm{s2}} \mathbf{F}_{\mathrm{p}}\right) + \lambda_s \,\mathrm{tr}(\mathbf{H}_{\mathrm{s1}} \mathbf{F}_{\mathrm{c}}) + 1\right) - \ln\left(\lambda_s \,\mathrm{tr}\left(\mathbf{H}_{\mathrm{s2}} \mathbf{F}_{\mathrm{p}}\right) + 1\right) \\ &= \max_{t_s>0} \varphi_s\left(\mathbf{F}_{\mathrm{p}}, \mathbf{F}_{\mathrm{c}}, t_s\right) \end{aligned} \tag{24}$$

where

$$\begin{aligned}\varphi_s\left(\mathbf{F}_\mathrm{p},\mathbf{F}_\mathrm{c},t_s\right) =& \ln\left(\lambda_s \operatorname{tr}\left(\mathbf{H}_{\mathrm{s}2}\mathbf{F}_\mathrm{p}\right)+\lambda_s \operatorname{tr}\left(\mathbf{H}_{\mathrm{s}1}\mathbf{F}_\mathrm{c}\right)+1\right)\\ &-t_s\left(\lambda_s \operatorname{tr}\left(\mathbf{H}_{\mathrm{s}2}\mathbf{F}_\mathrm{p}\right)+1\right)+\ln t_s+1\end{aligned} \tag{25}$$

Let $x=\lambda_e \operatorname{tr}(\mathbf{H}_{\mathrm{e}2}\mathbf{F}_\mathrm{c})+\lambda_e \operatorname{tr}\left(\mathbf{H}_{\mathrm{e}1}\mathbf{F}_\mathrm{p}\right)+1$ and $t=t_{ep}$; the, $R_{e,p}$ can be written as

$$\begin{aligned}R_{e,p}\ln 2 &= \ln\left(\lambda_e \operatorname{tr}(\mathbf{H}_{\mathrm{e}2}\mathbf{F}_\mathrm{c})+\lambda_e \operatorname{tr}\left(\mathbf{H}_{\mathrm{e}1}\mathbf{F}_\mathrm{p}\right)+1\right)-\ln(\lambda_e \operatorname{tr}(\mathbf{H}_{\mathrm{e}2}\mathbf{F}_\mathrm{c})+1)\\ &=\min_{t_{ep}>0}\varphi_{ep}\left(\mathbf{F}_\mathrm{p},\mathbf{F}_\mathrm{c},t_{ep}\right)\end{aligned} \tag{26}$$

where

$$\begin{aligned}\varphi_{ep}\left(\mathbf{F}_\mathrm{p},\mathbf{F}_\mathrm{c},t_{ep}\right) =& t_{ep}\left(\lambda_e \operatorname{tr}(\mathbf{H}_{\mathrm{e}2}\mathbf{F}_\mathrm{c})+\lambda_e \operatorname{tr}\left(\mathbf{H}_{\mathrm{e}1}\mathbf{F}_\mathrm{p}\right)+1\right)\\ &-\ln t_{ep}-1-\ln(\lambda_e \operatorname{tr}(\mathbf{H}_{\mathrm{e}2}\mathbf{F}_\mathrm{c})+1)\end{aligned} \tag{27}$$

Let $x=\lambda_e \operatorname{tr}\left(\mathbf{H}_{\mathrm{e}1}\mathbf{F}_\mathrm{p}\right)+\lambda_e \operatorname{tr}(\mathbf{H}_{\mathrm{e}2}\mathbf{F}_\mathrm{c})+1$, $t=t_{es}$, $R_{e,s}$ can be written as

$$\begin{aligned}R_{e,s}\ln 2 &= \ln\left(\lambda_e \operatorname{tr}\left(\mathbf{H}_{\mathrm{e}1}\mathbf{F}_\mathrm{p}\right)+\lambda_e \operatorname{tr}(\mathbf{H}_{\mathrm{e}2}\mathbf{F}_\mathrm{c})+1\right)-\ln\left(\lambda_e \operatorname{tr}\left(\mathbf{H}_{\mathrm{e}1}\mathbf{F}_\mathrm{p}\right)+1\right)\\ &=\min_{t_{es}>0}\varphi_{es}\left(\mathbf{F}_\mathrm{p},\mathbf{F}_\mathrm{c},t_{es}\right)\end{aligned} \tag{28}$$

where,

$$\begin{aligned}\varphi_{es}\left(\mathbf{F}_\mathrm{p},\mathbf{F}_\mathrm{c},t_{es}\right) =& t_{es}\left(\lambda_e \operatorname{tr}\left(\mathbf{H}_{\mathrm{e}1}\mathbf{F}_\mathrm{p}\right)+\lambda_e \operatorname{tr}(\mathbf{H}_{\mathrm{e}2}\mathbf{F}_\mathrm{c})+1\right)\\ &-\ln t_{es}-1-\ln\left(\lambda_e \operatorname{tr}\left(\mathbf{H}_{\mathrm{e}1}\mathbf{F}_\mathrm{p}\right)+1\right)\end{aligned} \tag{29}$$

By applying the semidefinite relaxation (SDR), we relax the rank($\mathbf{F}_\mathrm{p}$) = rank($\mathbf{F}_\mathrm{c}$) = 1 constraint and apply Dinklbach's algorithm [24]. Then, subproblem (P1.1) can be written as

$$\max_{\mathbf{f}_\mathrm{p},\mathbf{f}_\mathrm{c},t_p,t_{es},t_{ep}} \quad \eta \tag{30}$$

$$s.t. \quad \mathbf{F}_\mathrm{c}\succcurlyeq 0,\mathbf{F}_\mathrm{p}\succcurlyeq 0 \tag{30a}$$

$$\operatorname{tr}(\mathbf{F}_\mathrm{c})\le P_c^{\max},\operatorname{tr}\left(\mathbf{F}_\mathrm{p}\right)\le P_p^{\max} \tag{30b}$$

$$t_s>0,t_p>0,t_{es}>0,t_{ep}>0 \tag{30c}$$

where $g\left(\mathbf{F}_\mathrm{c},\mathbf{F}_\mathrm{p}\right)=\frac{\left(\varphi_p\left(\mathbf{F}_\mathbf{p},\mathbf{F}_\mathbf{c},t_p\right)-\varphi_{ep}\left(\mathbf{F}_\mathrm{p},\mathbf{F}_\mathrm{c},t_{ep}\right)+\varphi_s\left(\mathbf{F}_\mathbf{p},\mathbf{F}_\mathbf{c},t_s\right)-\varphi_{es}\left(\mathbf{F}_\mathrm{p},\mathbf{F}_\mathrm{c},t_{es}\right)\right)}{\ln 2}$, where ρ is the auxiliary variable introduced by applying Dinkelbach's algorithm to solve this fractional programming problem. It can be shown that (P1.1) is convex for $\left(\mathbf{F}_\mathrm{p},\mathbf{F}_\mathrm{c}\right)$ or $\left(t_s,t_p,t_{es},t_{ep}\right)$. Therefore, it can be solved by applying alternating optimization techniques. According to Lemma 1, the optimal $\left(\mathbf{F}_\mathrm{p},\mathbf{F}_\mathrm{c}\right)$ for fixed $\left(t_s,t_p,t_{es},t_{ep}\right)$ can be derived in closed form as follows:

$${t_p}^*=\left(\lambda_p \operatorname{tr}\left(\mathbf{H}_{\mathrm{p}2}\mathbf{F}_\mathrm{c}\right)+1\right)^{-1} \tag{31}$$

$${t_s}^*=\left(\lambda_s \operatorname{tr}\left(\mathbf{H}_{\mathrm{s}2}\mathbf{F}_\mathrm{p}\right)+1\right)^{-1} \tag{32}$$

$${t_{es}}^*=\left(\lambda_e \operatorname{tr}\left(\mathbf{H}_{\mathrm{e}1}\mathbf{F}_\mathrm{p}\right)+\lambda_e \operatorname{tr}(\mathbf{H}_{\mathrm{e}2}\mathbf{F}_\mathrm{c})+1\right)^{-1} \tag{33}$$

$${t_{ep}}^*=\left(\lambda_e \operatorname{tr}(\mathbf{H}_{\mathrm{e}2}\mathbf{F}_\mathrm{c})+\lambda_e \operatorname{tr}\left(\mathbf{H}_{\mathrm{e}1}\mathbf{F}_\mathrm{p}\right)+1\right)^{-1} \tag{34}$$

On the other hand, for a given $\left({t_p}^*,{t_s}^*,{t_{es}}^*,{t_{ep}}^*\right)$, the optimal $\left(\mathbf{F}_\mathrm{p},\mathbf{F}_\mathrm{c}\right)$ is solved by each fixed $\left({t_p}^*,{t_s}^*,{t_{es}}^*,{t_{ep}}^*\right)$ iteration. Since (P1.1) is convex, it can be solved efficiently by using a convex optimization solver (e.g., CVX), and, eventually, the optimal solution is obtained by alternately updating $\left(\mathbf{F}_\mathrm{p},\mathbf{F}_\mathrm{c}\right)$ and $\left({t_p}^*,{t_s}^*,{t_{es}}^*,{t_{ep}}^*\right)$. Note that the obtained $\mathbf{F}_\mathrm{c}$ and $\mathbf{F}_\mathrm{p}$ are not guaranteed to be rank 1 matrices because the rank 1 constraint is discarded in (P1.2) by applying SDR. To solve the omitted constraint rank equal to 1, we apply a Gaussian randomization method reduction, the details of which are omitted here for the sake of brevity. Algorithm 1 is summarized as follows.

Algorithm 1 Alternating optimization solves P1.1

Input: $P_c^{\max}, P_p^{\max}, \mathbf{H}_{\mathrm{p1}}, \mathbf{H}_{\mathrm{p2}}, \mathbf{H}_{\mathrm{s1}}, \mathbf{H}_{\mathrm{s2}}, \mathbf{H}_{\mathrm{e1}}, \mathbf{H}_{\mathrm{e2}}, \lambda_p, \lambda_s, \lambda_e, I_{th}$
Output: $\mathbf{f}_{\mathrm{c}}, \mathbf{f}_{\mathrm{p}}$
Initialize: $\mathbf{f}_{\mathrm{c}}, \mathbf{f}_{\mathrm{p}}$ according to the transmitted power constraint
Set up: $\rho = 0,\ \mathrm{m} = 1, \mathcal{E}, M_{\max}, \mathbf{F}_{\mathrm{c}}^{(0)} = \mathbf{f}_{\mathrm{c}}\mathbf{f}_{\mathrm{c}}^H, \mathbf{F}_{\mathrm{p}}^{(0)} = \mathbf{f}_{\mathrm{p}}\mathbf{f}_{\mathrm{p}}^H, \quad g\left(\mathbf{F}_{\mathrm{c}}, \mathbf{F}_{\mathrm{p}}\right)$
repeat
  repeat
    Given $\mathbf{F}_{\mathrm{c}}^{(\mathrm{m}-1)}$ and $\mathbf{F}_{\mathrm{p}}^{(\mathrm{m}-1)}$, find the optimal $t_p^{(\mathrm{m})}, t_s^{(\mathrm{m})}, t_{es}^{(\mathrm{m})}, t_{ep}^{(\mathrm{m})}$according to (31)(32)(33)(34).
    Given $t_p^{(\mathrm{m})}, t_s^{(\mathrm{m})}, t_{es}^{(\mathrm{m})}, t_{ep}^{(\mathrm{m})}$, the optimal values of $(\mathbf{F}_{\mathrm{p}}, \mathbf{F}_{\mathrm{c}})$ are solved by CVX.
    Update $m = m + 1$.
    Until the target value converges.
  until;
  Record Calculation $\rho^{(0)} = g\left(\mathbf{F}_{\mathrm{c}}^{(0)}, \mathbf{F}_{\mathbf{p}}^{(0)}\right) / P_{\text{total}}{}^{(0)}$.
  If $g\left(\mathbf{F}_{\mathrm{c}}, \mathbf{F}_{\mathrm{p}}\right) - \rho P_{\text{total}} \leq \varepsilon$ **then** set $Flag = 1$ and break
  else
    Set $Flag = 0, \rho^{(m+1)} = g\left(\mathbf{F}_{\mathrm{c}}^{(\mathrm{m})}, \mathbf{F}_{\mathrm{p}}^{(\mathrm{m})}\right) / P_{\text{total}}^{(\mathrm{m})}$ and $m = m + 1$.
  end if
  Until $Flag = 1$ or $m = M_{\max}$.
until;

3.2. Given $\left(\mathbf{f}_{\mathrm{c}}, \mathbf{f}_{\mathrm{p}}\right)$, Optimize $\boldsymbol{\Phi}$

First, we let $\mathbf{v} = \left[e^{j\theta_1}, \ldots, e^{j\theta_n}\right]^H$; then, $\boldsymbol{\Phi} = \operatorname{diag}\left(e^{j\theta_1}, \ldots, e^{j\theta_n}\right) = \operatorname{diag}\left(\mathbf{v}^H\right)$.
Let $\overline{\mathbf{v}} = \left[1, \mathbf{v}^H\right]^H, \mathbf{V} = \overline{\mathbf{v}}\overline{\mathbf{v}}^H$. And we define the following symbols below:

$$\boldsymbol{T}_{p1} = \begin{bmatrix} \mathbf{h}_{\mathrm{pp}}^H \\ \operatorname{diag}\left(\mathbf{h}_{\mathrm{rp}}^H\right)\mathbf{G}_{\mathrm{p}} \end{bmatrix} \mathbf{f}_{\mathrm{p}}\mathbf{f}_{\mathrm{p}}^H \begin{bmatrix} \mathbf{h}_{\mathrm{pp}}^H \\ \operatorname{diag}\left(\mathbf{h}_{\mathrm{rp}}^H\right)\mathbf{G}_{\mathrm{p}} \end{bmatrix}^H,$$

$$\boldsymbol{T}_{p2} = \begin{bmatrix} \mathbf{h}_{\mathrm{cp}}^H \\ \operatorname{diag}\left(\mathbf{h}_{\mathrm{rp}}^H\right)\mathbf{G}_{\mathrm{c}} \end{bmatrix} \mathbf{f}_{\mathrm{c}}\mathbf{f}_{\mathrm{c}}^H \begin{bmatrix} \mathbf{h}_{\mathrm{cp}}^H \\ \operatorname{diag}\left(\mathbf{h}_{\mathrm{rp}}^H\right)\mathbf{G}_{\mathrm{c}} \end{bmatrix}^H,$$

$$\boldsymbol{T}_{s1} = \begin{bmatrix} \mathbf{h}_{\mathrm{cs}}^H \\ \operatorname{diag}\left(\mathbf{h}_{\mathrm{rs}}^H\right)\mathbf{G}_{\mathrm{c}} \end{bmatrix} \mathbf{f}_{\mathrm{c}}\mathbf{f}_{\mathrm{c}}^H \begin{bmatrix} \mathbf{h}_{\mathrm{cs}}^H \\ \operatorname{diag}\left(\mathbf{h}_{\mathrm{rs}}^H\right)\mathbf{G}_{\mathrm{c}} \end{bmatrix}^H,$$

$$\boldsymbol{T}_{s2} = \begin{bmatrix} \mathbf{h}_{\mathrm{ps}}^H \\ \operatorname{diag}\left(\mathbf{h}_{\mathrm{rs}}^H\right)\mathbf{G}_{\mathrm{p}} \end{bmatrix} \mathbf{f}_{\mathrm{p}}\mathbf{f}_{\mathrm{p}}^H \begin{bmatrix} \mathbf{h}_{\mathrm{ps}}^H \\ \operatorname{diag}\left(\mathbf{h}_{\mathrm{rs}}^H\right)\mathbf{G}_{\mathrm{p}} \end{bmatrix}^H,$$

$$\boldsymbol{T}_{e1} = \begin{bmatrix} \mathbf{h}_{\mathrm{pe}}^H \\ \operatorname{diag}\left(\mathbf{h}_{\mathrm{re}}^H\right)\mathbf{G}_{\mathrm{p}} \end{bmatrix} \mathbf{f}_{\mathrm{p}}\mathbf{f}_{\mathrm{p}}^H \begin{bmatrix} \mathbf{h}_{\mathrm{pe}}^H \\ \operatorname{diag}\left(\mathbf{h}_{\mathrm{re}}^H\right)\mathbf{G}_{\mathrm{p}} \end{bmatrix}^H,$$

$$\boldsymbol{T}_{e2} = \begin{bmatrix} \mathbf{h}_{\mathrm{ce}}^H \\ \operatorname{diag}\left(\mathbf{h}_{\mathrm{re}}^H\right)\mathbf{G}_{\mathrm{c}} \end{bmatrix} \mathbf{f}_{\mathrm{c}}\mathbf{f}_{\mathrm{c}}^H \begin{bmatrix} \mathbf{h}_{\mathrm{ce}}^H \\ \operatorname{diag}\left(\mathbf{h}_{\mathrm{re}}^H\right)\mathbf{G}_{\mathrm{c}} \end{bmatrix}^H.$$

According to Lemma 1, we can obtain

$$\begin{aligned} \ln 2R_p &= \ln\left(\lambda_p \operatorname{tr}\left(\mathbf{T}_{\mathrm{p1}}\mathbf{V}\right) + \lambda_p \operatorname{tr}\left(\mathbf{T}_{\mathrm{p2}}\mathbf{V}\right) + 1\right) - \ln\left(\lambda_p \operatorname{tr}\left(\mathbf{T}_{\mathbf{p2}}\mathbf{V}\right) + 1\right) \\ &= \max_{u_p > 0} \psi_p\left(\mathbf{V}, u_p\right) \end{aligned} \tag{35}$$

where

$$\psi_p\left(\mathbf{V}, u_p\right) = \ln\left(\lambda_p \operatorname{tr}\left(\mathbf{T}_{\mathrm{p1}}\mathbf{V}\right) + \lambda_p \operatorname{tr}\left(\mathbf{T}_{\mathrm{p2}}\mathbf{V}\right) + 1\right) - u_p\left(\lambda_p \operatorname{tr}\left(\mathbf{T}_{\mathrm{p2}}\mathbf{V}\right) + 1\right) + \ln u_p + 1 \tag{36}$$

Similarly,

$$\begin{aligned} \ln 2R_s &= \ln(\lambda_s \operatorname{tr}(\mathbf{T}_{s1}\mathbf{V}) + \lambda_s \operatorname{tr}(\mathbf{T}_{\mathbf{s2}}\mathbf{V}) + 1) - \ln(\lambda_s \operatorname{tr}(\mathbf{T}_{\mathrm{s2}}\mathbf{V}) + 1) \\ &= \max_{u_s > 0} \psi_s(\mathbf{V}, u_s) \end{aligned} \tag{37}$$

where

$$\psi_s(\mathbf{V}, u_s) = \ln(\lambda_s \operatorname{tr}(\mathbf{T}_{s1}\mathbf{V}) + \lambda_s \operatorname{tr}(\mathbf{T}_{s2}\mathbf{V}) + 1) - u_s(\lambda_s \operatorname{tr}(\mathbf{T}_{s2}\mathbf{V}) + 1) + \ln u_s + 1 \tag{38}$$

$$\begin{aligned} \ln 2R_{ep} &= \ln(\lambda_e \operatorname{tr}(\mathbf{T}_{e1}\mathbf{V}) + \lambda_e \operatorname{tr}(\mathbf{T}_{e2}\mathbf{V}) + 1) - \ln(\lambda_e \operatorname{tr}(\mathbf{T}_{e2}\mathbf{V}) + 1) \\ &= \min_{u_{ep}>0} \psi_{ep}(\mathbf{V}, u_{ep}) \end{aligned} \tag{39}$$

where

$$\psi_{ep}(\mathbf{V}, u_{ep}) = u_{ep}(\lambda_e \operatorname{tr}(\mathbf{T}_{e1}\mathbf{V}) + \lambda_e \operatorname{tr}(\mathbf{T}_{e2}\mathbf{V}) + 1) - \ln u_{ep} - 1 - \ln(\lambda_e \operatorname{tr}(\mathbf{T}_{e2}\mathbf{V}) + 1) \tag{40}$$

$$\begin{aligned} \ln 2R_{es} &= \ln(\lambda_e \operatorname{tr}(\mathbf{T}_{e1}\mathbf{V}) + \lambda_e \operatorname{tr}(\mathbf{T}_{e2}\mathbf{V}) + 1) - \ln(\lambda_e \operatorname{tr}(\mathbf{T}_{e1}\mathbf{V}) + 1) \\ &= \min_{u_{es}>0} \psi_{es}(\mathbf{V}, u_{es}) \end{aligned} \tag{41}$$

where

$$\psi_{es}(\mathbf{V}, u_{es}) = u_{es}(\lambda_e \operatorname{tr}(\mathbf{T}_{e1}\mathbf{V}) + \lambda_e \operatorname{tr}(\mathbf{T}_{e2}\mathbf{V}) + 1) - \ln u_{es} - 1 - \ln(\lambda_e \operatorname{tr}(\mathbf{T}_{e1}\mathbf{V}) + 1) \tag{42}$$

By the semidefinite relaxation (SDR) method, we relax the $\operatorname{rank}(\mathbf{V}) = 1$ constraint, and the subproblem of (P1.2) can be written as follows:

$$\max_{u_p, u_s, u_{ep}, u_{es}} \quad \psi_p(\mathbf{V}, u_p) - \psi_{ep}(\mathbf{V}, u_{ep}) + \psi_s(\mathbf{V}, u_s) - \psi_{es}(\mathbf{V}, u_{es}) \tag{43}$$

$$s.t. \quad \mathbf{V} \succcurlyeq 0 \tag{43a}$$

$$\operatorname{diag}(\mathbf{V}) = 1 \tag{43b}$$

$$\operatorname{tr}(\mathbf{T}_{p2}\mathbf{V}) \leq I_{th} \tag{43c}$$

$$u_p > 0, u_s > 0, u_{ep} > 0, u_{es} > 0 \tag{43d}$$

It can be shown that (P1.2) is convex for $\mathbf{V}$ or $(u_p, u_s, u_{ep}, u_{es})$. Therefore, it can be solved by applying alternating optimization techniques. According to Lemma 1, the optimal $(u_p, u_s, u_{ep}, u_{es})$ for a fixed $\mathbf{V}$ can be derived in closed form as follows:

$$u_p^* = \left(\lambda_p \operatorname{tr}(\mathbf{T}_{p2}\mathbf{V}) + 1\right)^{-1} \tag{44}$$

$$u_s{}^* = \left(\lambda_s \operatorname{tr}(\mathbf{T}_{s2}\mathbf{V}) + 1\right)^{-1} \tag{45}$$

$$u_{ep}^* = \left(\lambda_e \operatorname{tr}(\mathbf{T}_{e1}\mathbf{V}) + \lambda_e \operatorname{tr}(\mathbf{T}_{e2}\mathbf{V}) + 1\right)^{-1} \tag{46}$$

$$u_{es}^* = \left(\lambda_e \operatorname{tr}(\mathbf{T}_{e2}\mathbf{V}) + \lambda_e \operatorname{tr}(\mathbf{T}_{e1}\mathbf{V}) + 1\right)^{-1} \tag{47}$$

For a given $(u_p{}^*, u_s{}^*, u_{ep}{}^*, u_{es}{}^*)$, the optimal $\mathbf{V}$ can be solved iteratively. The overall solution method is similar to the subproblem (P1.1), which is finally solved with the help of the CVX tool. The complete Algorithm 2 for solving the entire problem is as follows.

Algorithm 2 Alternating optimization solves P1

Input: $P_c^{\max}, P_p^{\max}, \mathbf{H}_{p1}, \mathbf{H}_{p2}, \mathbf{H}_{s1}, \mathbf{H}_{s2}, \mathbf{H}_{e1}, \mathbf{H}_{e2}, \lambda_p, \lambda_s, \lambda_e$
$\mathbf{T}_{p1}, \mathbf{T}_{p2}, \mathbf{T}_{s1}, \mathbf{T}_{s2}, \mathbf{T}_{e1}, \mathbf{T}_{e2}, \varepsilon, L$

Output: $\mathbf{f}_c, \mathbf{f}_p, \mathbf{v}$

Initialize: the reflection coefficient matrix $\mathbf{\Phi}^{(0)}, \mathbf{v}^{(0)}$

Set up: $l = 1$

repeat

Apply Algorithm 1 to solve (P1.1) for a given $\mathbf{v}^{(l-1)}$ and denote it as $\mathbf{f}_c{}^{(l)}, \mathbf{f}_p{}^{(l)}$.

For a given $\mathbf{f}_c{}^{(l)}, \mathbf{f}_p{}^{(l)}$, solve (P1.2) and express it as $\bar{\mathbf{v}}^{(l)}$.

Recover $\mathbf{v}^{(l)}$ from $\bar{\mathbf{v}}^{(l)}$ using Gaussian randomization algorithm.

Update $l = l + 1$.

until the target value of (P1) converges to ε or $l = l + 1$.

until;

3.3. Algorithm Complexity

The overall algorithm for solving the problem is shown in Algorithm 2. The complexity of the algorithm comes from solving the two subproblems (P1.1) and (P1.2), the complexity of the algorithm in solving $\mathbf{f}_c, \mathbf{f}_p$ is $\mathcal{O}\left(M_c^{4.5} + M_p^{4.5}\right)$, and the complexity of the algorithm in solving $\mathbf{v}$ is $\mathcal{O}\left((N+1)^{4.5}\right)$ [25]. Assuming that the number of iterations in the two subproblems are L_1 and L_2, the complexity is $\mathcal{O}\left(L_1\left(M_c^{4.5} + M_p^{4.5}\right)\right)$ and $\mathcal{O}\left(L_2(N+1)^{4.5}\right)$, respectively. Thus, we know that the number of iterations in the overall iterative process is L_3, and the complexity of the whole algorithm is $\mathcal{O}\left(L_3\left(L_1\left(M_c^{4.5} + M_p^{4.5}\right) + L_2(N+1)^{4.5}\right)\right)$.

4. Simulation Results

In this section, the effectiveness of the algorithm in this system model problem scenario is demonstrated by comparing it with the scheme without RIS and the RIS random phase algorithm scheme. We assume that the locations of primary user PU and secondary user SU are (100, 20) and (50, 0), respectively, the locations of PBS and CBS are (150, 0) and (0, 0), respectively, the locations of RIS and Eve are (50, 30), (100, −10), respectively, and the noise variance σ^2 is set to 10^{-10} W. The path loss of all channels is given by the equation $L(d_{ab}) = \sqrt{L_0(d_{ab}/d_0)^{-\alpha_{ab}}}$, where L_0 denotes the path loss at the reference distance $d_0 = 1$ m, d denotes the straight-line distance from communication end a to communication end b, α is the path loss exponent, and the path loss coefficients of PBS to RIS, CBS to RIS, RIS to PU, RIS to SU, Eve to RIS, PBS to PU, PBS to SU, CBS to PU, CBS to SU, PBS to Eve, and CBS to Eve have path loss coefficients of $\alpha_{PR} = \alpha_{CR} = 2, \alpha_{RP} = \alpha_{RS} = \alpha_{ER} = 2.6$, and $\alpha_{PP} = \alpha_{PS} = \alpha_{CP} = \alpha_{CS} = \alpha_{PE} = \alpha_{CE} = 3.5$, respectively.

It is assumed that the small-scale fading of the channels from PBS to RIS, RIS to PU, CBS to RIS, RIS to SU, and Eve to RIS all follow the Rayleigh fading model. The small-scale fading is expressed in the form of the equation $g_{ab} = \sqrt{\beta/1+\beta}g_{ab}^{LOS} + \sqrt{\beta/1+\beta}g_{ab}^{NLOS}$, where β denotes the Rician factor, and g_{ab}^{LOS} and g_{ab}^{NLOS} represent the deterministic line-of-sight component and non-deterministic line-of-sight component of the channel of interest between the a and b ends, respectively. Other specific parameters are set as follows (Table 1).

Table 1. Parameter setting.

Parameters	Values
Path loss L_0	-30 dB
Rician factor β	$\beta = 10$
QoS	2 bps/Hz
Hardware power loss	$P_{su}^{cir} = P_{pu}^{cir} = 0.005$
	$P_{BS}^{cir} = 1.5$
	$P_{sta} = 0.1$
	$P_{dyn} = 0.0001$
Other parameters	$\varepsilon = 0.001 \quad L = 20$

Figure 2 shows the variation of the safety energy efficiency with the number of CBS antennas for different schemes with a fixed number of PBS base station antennas $M_c = 3$, with a maximum transmit power of 30 dBm, and a number of RISs $N = 16$. Figure 3 shows the variation of different schemes with a fixed number of CBS base station antennas. It can be seen that, with the increase in the number of antennas, the system safety performance is improved to a certain extent, and the proposed algorithm is better than the other two schemes. In addition, the system with random RIS assistance is slightly better than the system without RIS assistance in terms of safety energy efficiency gain.

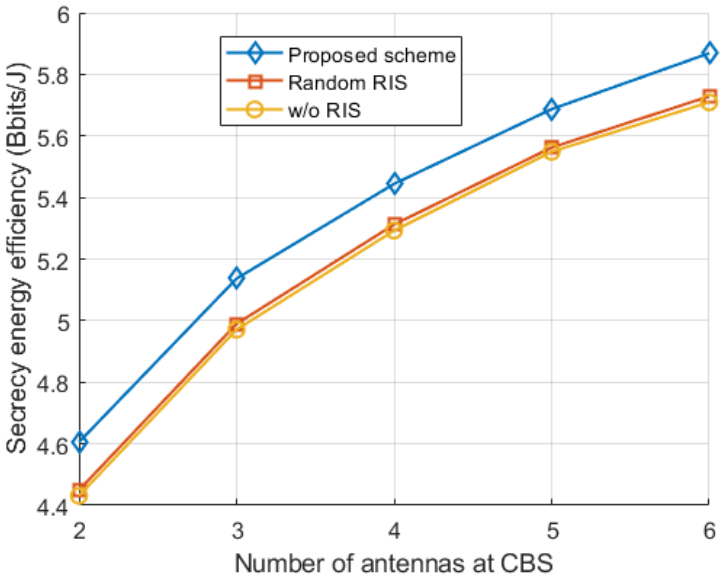

Figure 2. SEE versus the CBS antennas.

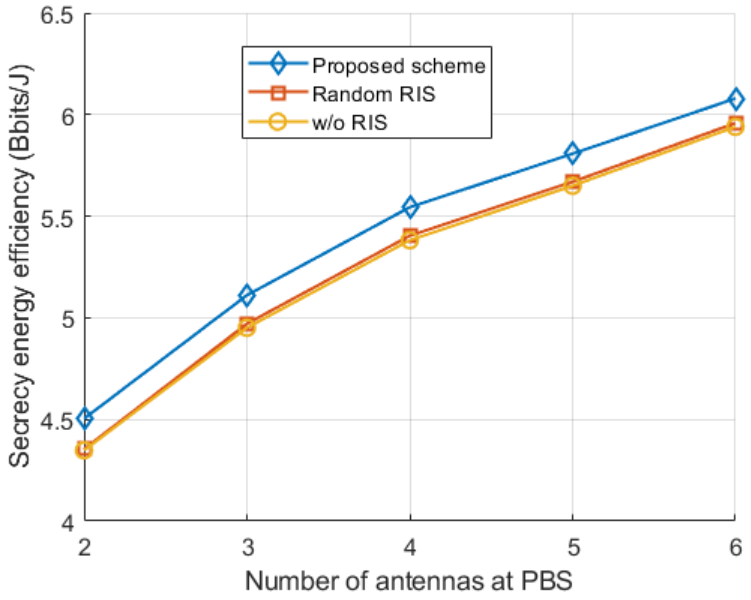

Figure 3. SEE versus the PBS antennas.

The convergence of the algorithm in this paper when $P_p^{\max} = P_c^{\max} = 30$ dBm is given in Figure 4. It can be seen that, as the number of iterations increases, the safety energy efficiency of the system increases monotonically until it maintains a steady state, which proves the effectiveness of the algorithm. Moreover, the more RIS reflection units, the greater the convergence value, which can be explained by the fact that the greater the number of RIS elements, the stronger the reflection of the signal in the expected direction.

Figure 5 shows the variation of the average security energy efficiency with the number of RIS reflective elements N for different schemes with a fixed number of base station antennas. At this time, the $P_{\max}$ is 30 dBm, the number of antennas of both base stations is 4, and the interference temperature threshold is I_{th} −90 dBm. From the figure, it can be seen that, with the increase in the number of RIS reflector units in a certain range, the security energy efficiency of the two schemes—our proposed scheme and the RIS random phase-shift—becomes larger, whereas the security energy efficiency of the scheme without the assistance of the RIS remains unchanged. By increasing the number of RIS reflector units, the RIS gains more flexibility in channel design for the PBS/CBS–RIS–PU/SU link.

This increased flexibility leads to improved beamforming gain. And the more RIS elements in the communication system, the more signal paths and energy the RIS reflects to improve the signal quality of the PUs and SUs while reducing the signal quality of the eavesdropper. However, it is worth noting that increasing the number of RISs is beneficial to improve the security energy efficiency of the whole communication system only within a certain range.

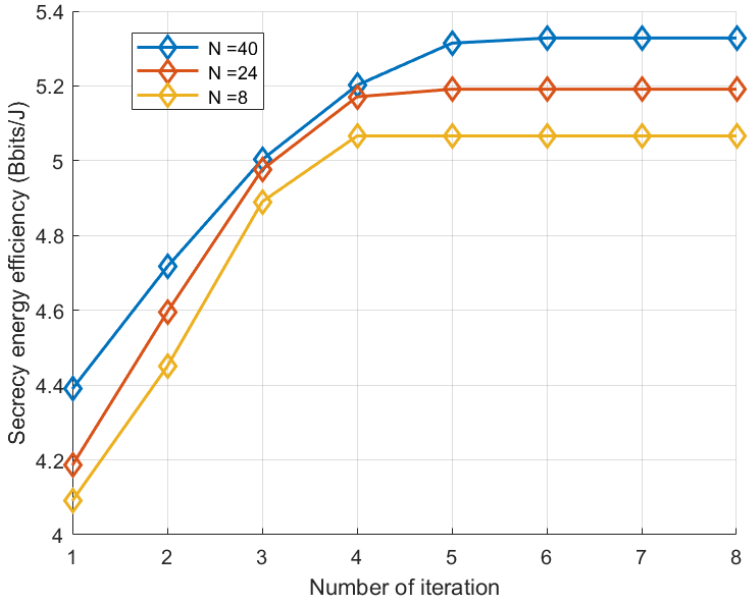

Figure 4. Convergence of the proposed algorithm.

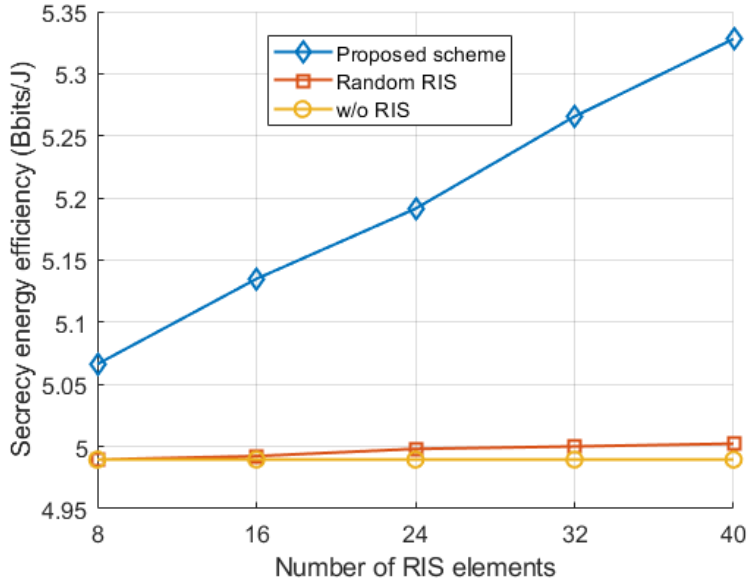

Figure 5. SEE versus the number of reflecting elements N.

Figures 6 and 7 show the variation of the security energy efficiency with CBS and PBS transmitting power for different schemes for N = 16. It can be observed that the gain effect of the proposed algorithm is significantly better than the other two schemes at different transmission powers. In addition, the safety energy efficiency of the three schemes gradually increases and then slowly decreases as the transmitted power $P_{\max}$ gradually increases. Because the applied scheme optimizes the phase shift of the RIS reflection unit, it harnesses the additional degrees of freedom in the channel, resulting in a gradual increase in the safety energy efficiency of the system. This is achieved despite the associated increase in energy consumption as the maximum power ($P_{\max}$) gradually

increases. As $P_{\max}$ increases further, the increase in system energy consumption dominates the system energy efficiency performance, leading to a decrease in safety energy efficiency. As $P_{\max}$ increases even further, the increased system rate begins to dominate the system safety energy efficiency, leading to a slow start of the decrease. Overall, the applied scheme is significantly better than the other two schemes.

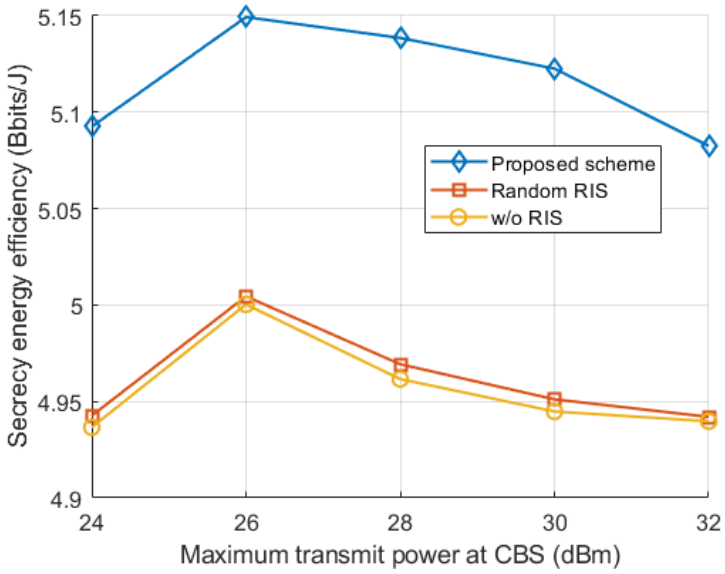

Figure 6. SEE versus CBS's maximum transmit power $P_{CBS}^{\max}$.

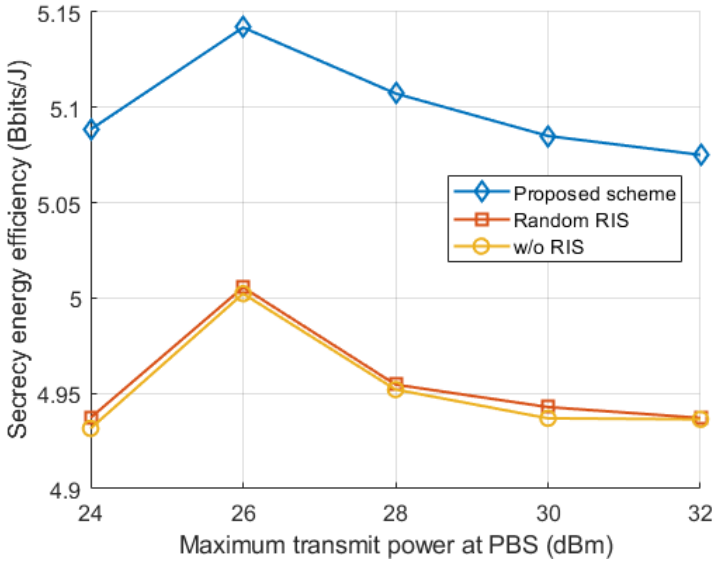

Figure 7. SEE versus CBS maximum transmit power $P_{PBS}^{\max}$.

Figure 8 shows the variation of the system safe energy efficiency for different I_{th} thresholds. As can be seen from the figure, the safe energy efficiency of all schemes is improved with the gradual increase in I_{th}. This is because the interference tolerance of the PU is greater when the interference temperature threshold I_{th} increases, which relaxes the constraints on the safe energy efficiency of the SU, and, thus, the safe energy efficiency of the whole communication system is improved. It can also be seen that the secure energy efficiency of our proposed scheme is significantly better than the benchmark scheme. Theoretically, the safe energy efficiency of the whole communication system should be saturated when the I_{th} increases to a certain value, which means that the interference temperature is no longer a factor affecting the safe energy efficiency of the system, which may be limited by the transmission power $P_{\max}$ or other factors.

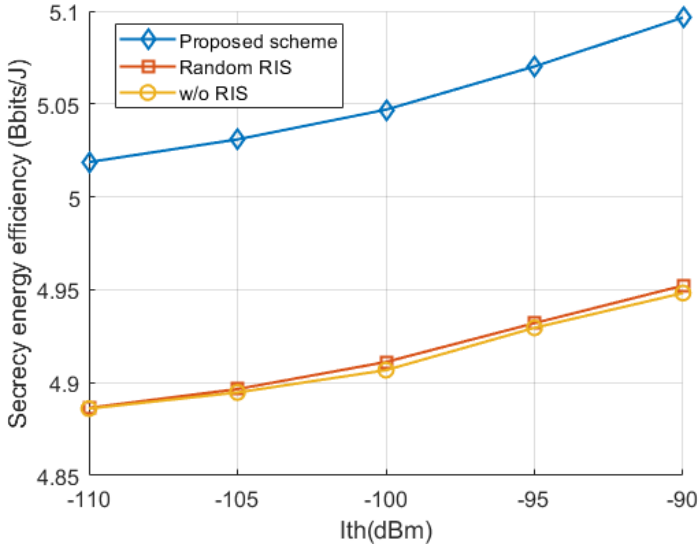

Figure 8. Variation of SEE with I_{th}.

Figure 9 shows the system safety energy efficiency versus the path loss between the RIS and the base station. Path loss being an important parameter in communication, it is obvious that a greater path loss causes the associated safe energy efficiency to gradually decrease. However, we can clearly notice from the figure that, for the same path loss parameter, the scheme with RIS is better than the scheme without RIS assistance. More importantly, our proposed scheme with phase-shift optimization for RIS is superior to the one with random phase-shift, which is due to the disordered nature of the random phase-shift of RIS, which appears to weaken the communication quality of the legitimate link. Overall, the simulation results demonstrate the superiority and necessity of our proposed scheme.

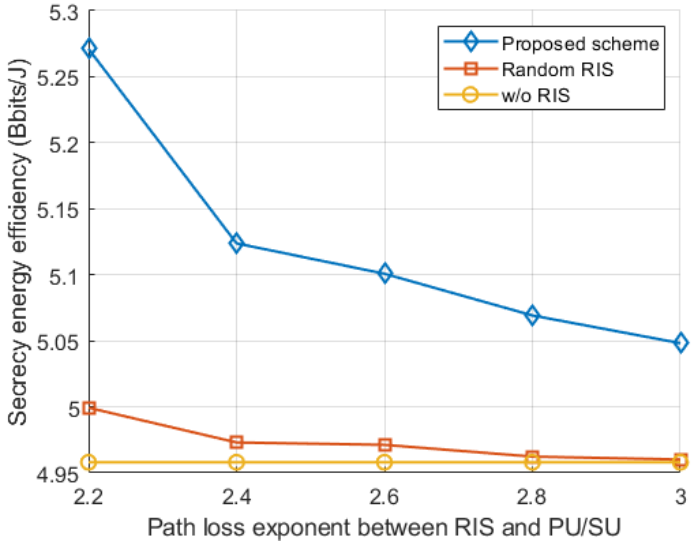

Figure 9. SEE versus path loss.

5. Conclusions

This paper addresses the issue of secure transmission in RIS-assisted MIMO CR systems. The system SEE maximization problem is studied by jointly optimizing the transmit beamforming at the PBS and CBS and the reflection phase shift matrix at the RIS, under the premise that the SU interference to the PU is limited to a predefined threshold. To tackle the complexity of the nonconvex problem, we propose an iterative alternating optimization algorithm that effectively decouples the original problem into two subproblems. Simulation

results show that the proposed algorithm can greatly improve the safe energy efficiency of the system, as a way to ensure the safe communication between PU and SU. Moreover, with the help of RIS, the SEE of the proposed algorithm is significantly improved compared to the benchmark solution.

Author Contributions: Conceptualization, X.W. (Xinshui Wang) and X.W. (Xu Wang); methodology, X.W. (Xinshui Wang); software, X.W. (Xu Wang), J.G. and Z.L.; validation, J.G., Z.L., X.L. and Y.M.; writing—original draft preparation, X.W. (Xinshui Wang) and X.W. (Xu Wang); writing—review and editing, X.W. (Xinshui Wang), X.W. (Xu Wang) and J.G. All authors have read and agreed to the published version of the manuscript.

Funding: This work was financially supported by the Natural Science Foundation of Shandong Province of China (Grant No. ZR2021MF013 and Grant No. ZR2021MF124).

Data Availability Statement: The data are not publicly available due to the data also forms part of an ongoing study.

Conflicts of Interest: The authors declare no conflicts of interest.

References

1. Huang, C.; Hu, S.; Alexandropoulos, G.C.; Zappone, A.; Yuen, C.; Zhang, R.; Di Renzo, M.; Debbah, M. Holographic MIMO Surfaces for 6G Wireless Networks: Opportunities, Challenges, and Trends. *IEEE Wirel. Commun.* **2020**, *27*, 118–125. [CrossRef]
2. Li, X.; Wang, Q.; Zeng, M.; Liu, Y.; Dang, S.; Tsiftsis, T.A.; Dobre, O.A. Physical-Layer Authentication for Ambient Backscatter-Aided NOMA Symbiotic Systems. *IEEE Trans. Commun.* **2023**, *71*, 2288–2303. [CrossRef]
3. Almohamad, A.; Tahir, A.M.; Al-Kababji, A.; Furqan, H.M.; Khattab, T.; Hasna, M.O.; Arslan, H. Smart and Secure Wireless Communications via Reflecting Intelligent Surfaces: A Short Survey. *IEEE Open J. Commun. Soc.* **2020**, *1*, 1442–1456. [CrossRef]
4. Huang, C.; Zappone, A.; Alexandropoulos, G.C.; Debbah, M.; Yuen, C. Reconfigurable intelligent surfaces for energy efficiency in wireless communication. *IEEE Trans. Wirel. Commun.* **2019**, *18*, 4157–4170. [CrossRef]
5. Chen, X.; Ng, D.W.K.; Gerstacker, W.H.; Chen, H.H. A Survey on Multiple-Antenna Techniques for Physical Layer Security. *IEEE Commun. Surv. Tutorials* **2017**, *19*, 1027–1053. [CrossRef]
6. Gui, G.; Liu, M.; Tang, F.; Kato, N.; Adachi, F. 6G: Opening New Horizons for Integration of Comfort, Security, and Intelligence. *IEEE Wirel. Commun.* **2020**, *27*, 126–132. [CrossRef]
7. Li, X.; Qi, H.; Do, D.T.; Hui, Z.; Ding, Y.; Zhu, M.; Peng, H. IQ-Impaired Wireless-Powered Modify-and-Forward Relaying for IoT Networks: An In-Depth Physical-Layer Security Analysis. *IEEE Internet Things J.* **2023**, *10*, 14912–14924. [CrossRef]
8. Feng, K.; Li, X.; Han, Y.; Jin, S.; Chen, Y. Physical Layer Security Enhancement Exploiting Intelligent Reflecting Surface. *IEEE Commun. Lett.* **2021**, *25*, 734–738. [CrossRef]
9. Li, X.; Zhang, J.; Han, C.; Hao, W.; Zeng, M.; Zhu, Z.; Wang, H. Reliability and Security of CR-STAR-RIS-NOMA Assisted IoT Networks. *IEEE Internet Things J.* **2023**. [CrossRef]
10. Pei, Y.; Liang, Y.C.; Zhang, L.; Teh, K.C.; Li, K.H. Achieving cognitive and secure transmissions using multiple antennas. In Proceedings of the IEEE 20th International Symposium on Personal, Indoor and Mobile Radio Communications, Tokyo, Japan, 13–16 September 2009; pp. 1–5.
11. Xiong, J.; Zhou, X.; Cao, K.; Liu, X.; Ma, D. Robust Secure Beamforming in Cognitive MIMO Wiretap Channels with Bounded Channel Errors. In Proceedings of the International Conference on Wireless Communications and Signal Processing (WCSP), Nanjing, China, 21–23 October 2020; pp. 742–747.
12. Al-Nahari, A.; Geraci, G.; Al-Jamali, M.; Ahmed, M.H.; Yang, N. Beamforming with Artificial Noise for Secure MISOME Cognitive Radio Transmissions. *IEEE Trans. Inf. Forensics Secur.* **2018**, *13*, 1875–1889. [CrossRef]
13. Mokari, N.; Parsaeefard, S.; Saeedi, H.; Azmi, P.; Hossain, E. Secure Robust Ergodic Uplink Resource Allocation in Relay-Assisted Cognitive Radio Networks. *IEEE Trans. Signal Process.* **2015**, *63*, 291–304. [CrossRef]
14. Alavi, F.; Mokari, N.; Saeedi, H. Secure resource allocation in OFDMA-based cognitive radio networks with two-way relays. In Proceedings of the 23rd Iranian Conference on Electrical Engineering, Tehran, Iran, 10–14 May 2015; pp. 171–176.
15. Chen, X.; Guo, L.; Li, X.; Dong, C.; Lin, J.; Mathiopoulos, P.T. Secrecy Rate Optimization for Cooperative Cognitive Radio Networks Aided by a Wireless Energy Harvesting Jammer. *IEEE Access* **2018**, *6*, 34127–34134. [CrossRef]
16. Zhang, L.; Wang, Y.; Tao, W.; Jia, Z.; Song, T.; Pan, C. Intelligent Reflecting Surface Aided MIMO Cognitive Radio Systems. *IEEE Trans. Veh. Technol.* **2020**, *69*, 11445–11457. [CrossRef]
17. Yuan, J.; Liang, Y.C.; Joung, J.; Feng, G.; Larsson, E.G. Intelligent Reflecting Surface (IRS)-Enhanced Cognitive Radio System. In Proceedings of the IEEE International Conference on Communications (ICC), Dublin, Ireland, 7–11 June 2020; pp. 1–6.
18. Dong, L.; Wang, H.M.; Xiao, H. Secure Cognitive Radio Communication via Intelligent Reflecting Surface. *IEEE Trans. Commun.* **2021**, *69*, 4678–4690. [CrossRef]
19. Zhang, X.; Li, A.; Guo, T. Secrecy Rate Maximization for IRS-assisted MISOME Cognitive Radio System. In Proceedings of the IEEE Wireless Communications and Networking Conference (WCNC), Austin, TX, USA, 10–13 April 2022; pp. 1958–1963.

20. Dong, L.; Wang, H.M.; Xiao, H.; Bai, J. Secure Intelligent Reflecting Surface Assisted MIMO Cognitive Radio Transmission. In Proceedings of the IEEE Wireless Communications and Networking Conference (WCNC), Nanjing, China, 29 March–1 April 2021; pp. 1–6.
21. Wu, X.; Ma, J.; Xing, Z.; Gu, C.; Xue, X.; Zeng, X. Secure and Energy Efficient Transmission for IRS-Assisted Cognitive Radio Networks. *IEEE Trans. Cogn. Commun. Netw.* **2022**, *8*, 170–185. [CrossRef]
22. Liu, L.; Zhang, R.; Chua, K.C. Secrecy Wireless Information and Power Transfer with MISO Beamforming. *IEEE Trans. Signal Process.* **2014**, *62*, 1850–1863. [CrossRef]
23. Li, Q.; Hong, M.; Wai, H.T.; Liu, Y.F.; Ma, W.K.; Luo, Z.Q. Transmit Solutions for MIMO Wiretap Channels using Alternating Optimization. *IEEE J. Sel. Areas Commun.* **2013**, *31*, 1714–1727. [CrossRef]
24. Dinkelbach, W. On nonlinear fractional programming. *Manag. Sci.* **1967**, *13*, 492–498. [CrossRef]
25. Polik, I.; Terlaky, T. Chapter 4—Interior point methods for nonlinear optimization. In *Nonlinear Optimization*, 1st ed.; Di Pillo, G., Schoen, F., Eds.; Springer: New York, NY, USA, 2010.